*SIMULATION OF SEMICONDUCTOR DEVICES AND PROCESSES Vol. 5*
Edited by S. Selberherr, H. Stippel, E. Strasser – September 1993


# Two-Dimensional Numerical Simulations of High Efficiency Silicon Solar Cells

G. Heiser, A. G. Aberle†, S. R. Wenham†, and M. A. Green†

School of Computer Science & Engineering, University of New South Wales
P.O.Box 1, Kensington, New South Wales, 2033, AUSTRALIA
†Centre for Photovoltaic Devices & Systems, University of New South Wales
P.O.Box 1, Kensington, New South Wales, 2033, AUSTRALIA

Abstract

This paper presents for the first time the use of two-dimensional (2D) device simulation for optimising design parameters of high-efficiency silicon solar cells of practical dimensions. We examine the influence of 2D effects on the operating conditions of these devices and give results for the optimal spacing of the front metal fingers. Numerical difficulties inherent in the simulations are being discussed.

## 1. Introduction

The *passivated emitter, rear locally-diffused* (PERL) silicon solar cell (Fig. 1) has recently been developed at the University of New South Wales (UNSW) and demonstrates record-high efficiencies of 23.2 % under non-concentrated ("one-sun") illumination [1]. It is estimated that PERL technology can yield efficiencies of up to 25 % if all design parameters are fully optimised. However, this requires improved understanding of the operating conditions of the devices. In this paper, state-of-the-art two-dimensional (2D) numerical simulation tools are for the first time applied to gain detailed insight into the operating conditions of practical high-efficiency Si solar cells and to optimise various design parameters.

## 2. Two-dimensional Effects in High-efficiency Silicon Solar Cells

One important design parameter of Si solar cells is the *front contact spacing*, i.e. the distance between the thin metal fingers contacting the emitter layer (the $n^+$ layer in a $n^+p$ structure). Since the metal contacts are opaque to light, a small finger spacing reduces cell efficiency due to excessively large shading losses. For wide spacings, however, the limited conductivity of the thin emitter layer leads to large resistive losses. Furthermore, the voltage drop resulting from the emitter resistance leads to an increased operating voltage half way between two metal fingers. This voltage profile results in increased electron concentrations in the central base region and a 2D electron flow in the base (Fig. 2).

In order to determine the optimum finger spacing by simulation, accurate modelling of the resistive losses in the emitter is essential. 1D simulations, which have been successfully used to optimise other design parameters (see e.g. [2]), cannot provide this accuracy, as they overestimate the emitter current due to the assumption of a vertical electron flow in the base (p layer). As a result of the 2D electron flow in the base the spacing of the front fingers can be increased well above the limits predicted by 1D models, and cell efficiency increases due to reduced shading losses as well as reduced metal contact recombination.

## 3. Difficulties and Limitations

High-efficiency Si solar cells are notoriously difficult to simulate. The main reason for this lies in the huge device dimensions (typical cells are 250 $\mu$m deep with a front contact spacing of 800 $\mu$m) and the large diffusion lengths (1–2 mm). Making use of symmetry, a simulation domain of 400 $\mu$m $\times$ 250 $\mu$m is therefore required. On the other hand, some dimensions of the cells are more typical for VLSI devices: the emitter depth is 1 $\mu$m, while the contact fingers are 3 $\mu$m wide. For a simplified cell with a planar front surface, a fully metallised back, and a $p^+$ "back surface field" (Fig. 2), there are 3 regions of the device which require, in at least one dimension, grid lines spaced 0.2 $\mu$m or less: the emitter (where roughly half of the incident light is absorbed), the back contact (where recombination is high), and the shade boundary under the front contact (where the generation rates are discontinuous). This easily leads to grid sizes which require massive supercomputer use.

The recently developed ETH device simulation package [3] allows the user to control grid densities well enough so that we could limit grid sizes to some 3,000-5,000 points (Fig. 3), which enabled us to perform the simulations on a Sun SPARC-2 workstation. However, the price to be paid for the small grid sizes is the poor condition of the linear systems that have to be solved in the course of the simulation. We found occasionally that some linear systems could not be solved by a direct solver, particularly on the Cray, which has a smaller mantissa length than machines using IEEE arithmetic. Iterative solvers have generally failed to converge on our problems. This is a serious restriction, as we are planning to investigate problems that require 3D simulations (cf. Sect. 5), which will only be possible if we can use iterative solvers. We are presently investigating the sources of these numerical problems and hope to solve them by the use of better adjusted grids.

| $n_{ie}$ *model* | oS | S | dA | BW | BW* |
|---|---|---|---|---|---|
| $n_i/10^{10}\,cm^{-3}$ | 1.548 | 1.247 | 1.493 | 1.09 | 1.00 |
| $P/P_{\mathrm{BW^*}}$ | 0.804 | 0.885 | 0.934 | 0.994 | 1.000 |

Table 1: Power output as a function of $n_i$

Another difficulty results from the extreme sensitivity of the cells to material properties such as minority carrier lifetimes and intrinsic carrier density, $n_i$. Table 1 shows the dependence of the simulated power output of a cell on the model used for $n_{ie}$ (effective $n_i$). The first four values in the table correspond to the models built into Simul [3], while the last one corresponds to model *BW* modified to yield $n_i = 1.00 \times 10^{10}\,cm^{-3}$, which is the value currently accepted in the photovoltaic community [4]. The results show that these models must be carefully tuned if the simulation results are to be compared with experimental data. In our simulations we used the BW* model and adjusted carrier lifetimes to 2 ms for good agreement with experimental data at a reference point (a finger spacing of 800$\mu m$).

## 4. Results

Fig. 4 shows the calculated electron flow in the base at the maximum power point of the solar cell of Fig. 2 (contact spacing of 800 $\mu$m) under long wavelength (1000 nm) illumination. The light intensity has been adjusted to yield the same short-circuit current as for standard white light of one-sun intensity (*AM1.5 spectrum*). As Si has an indirect bandgap of about 1.1 eV, light of such a wavelength is only very weakly absorbed and carrier generation is almost uniform throughout the device. The plot shows that the electron flow in the base has

indeed a significant lateral component. The effect is particularly pronounced for electrons generated near the back contact: These electrons move a considerable distance along the rear surface until they diffuse upwards to be collected by the emitter region. Consequently, a significant fraction of the electron current that otherwise would have to be transported by the emitter flows through the base of the cell. This effect reduces the current density and hence the ohmic losses in the emitter. However, due to the enhanced electron path length in the base, this 2D effect is only beneficial for solar cell efficiency if the electron diffusion length is larger than about half the front finger spacing.

Fig. 5 shows the corresponding electron density and the direction of the electron flow under AM1.5 illumination. The combination of weak absorption at long wavelengths and stronger absorption at shorter wavelengths shifts the area of maximum electron concentration closer to the front surface and results in an electron flow which, in most of the device, is more horizontal than vertical.

Fig. 6 shows that the optimum front finger spacing under AM1.5 illumination is about 1.1–1.2 mm, compared to 0.8–0.9 mm as predicted by 1D models. Interestingly, the 2D model predicts only a weak decrease of efficiency for wide finger spacings: According to Fig. 6, the power output drops only by 1.3 % if the finger spacing is increased from 1.1 to 2 mm, while the 1D model predicts an efficiency loss more than twice as big.

## 5. Conclusions and Future Work

The 2D simulations presented in this paper considerably improve the general understanding of the operating conditions of high-efficiency Si solar cells. Improved values for an important design parameter, the front finger spacing, have been obtained. We expect that these and forthcoming simulation results will help to further improve the efficiency of laboratory cells at UNSW. Presently we are working on the optimisation of the back contacts of PERL cells, which will involve 3D simulations.

## 6. Acknowledgments

This work was partially funded by a grant from the Australian Research Council (ARC). The Centre for Photovoltaic Devices and Systems is supported by the ARC's Special Research Centres Scheme and Pacific Power. A.G.A. gratefully acknowledges the support of a Feodor Lynen Fellowship provided by the Alexander von Humboldt Foundation. Finally, we would like to thank Wolfgang Fichtner from ETH Zürich for granting access to the latest versions of Simul and Kevin Kells and Ulrich Krumbein of his group for their help with various problems encountered in the simulations.

## References

[1] M. A. Green. Recent advances in silicon solar cell performance. In *Proc. 10th European Communities Photovoltaic Solar Energy Conf.*, p. 250, Lisbon, 1991.

[2] A. Aberle, W. Warta, J. Knobloch, and B. Voss. Surface passivation of high efficiency silicon solar cells. In *Proc. 21st IEEE Photovoltaic Specialists Conf.*, p. 233, Orlando, 1990.

[3] Integrated Systems Lab. *Simul Manual.* ETH Zürich, Switzerland, 1992.

[4] A. B. Sproul and M. A. Green. Improved value for the silicon intrinsic carrier concentration from 275 to 375 K. *J. App. Phys.*, 70:846–54, 1991.

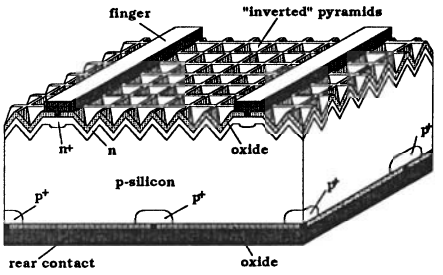


Figure 1: The UNSW PERL Si solar cell.

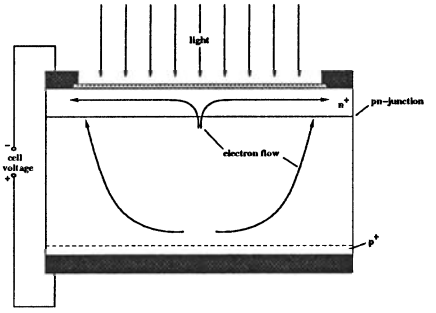


Figure 2: Schematic view of a simplified solar cell and the electron current flow within the device.

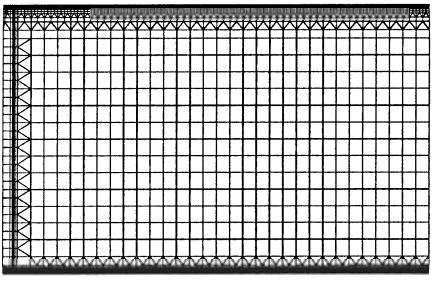

Figure 3: Simulation grid for the above cell. One emitter contact is at the top left corner of the picture, while the right edge coincides with the symmetry plane between two contacts

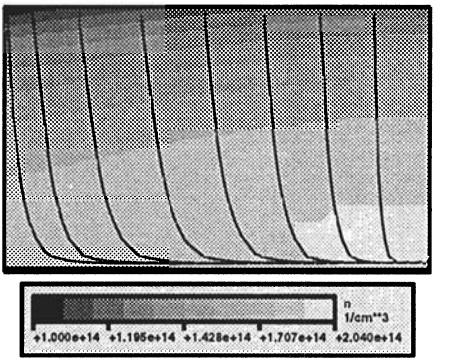


Figure 4: Electron density and electron flow lines under 1000 nm illumination.

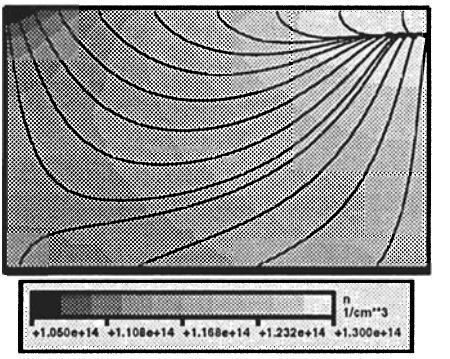


Figure 5: Electron density and electron flow lines under AM1.5 illumination.

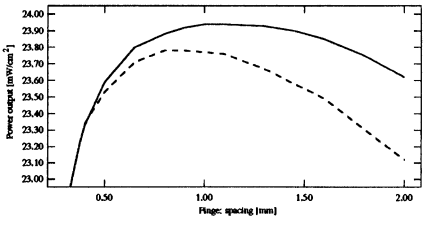


Figure 6: Output power according to 1D (broken line) and 2D (solid line) simulations under AM1.5 illumination.